COMSERVA
JURNAL PENELITIAN DAN PENGABDIAN MASYARAKAT
Volume 4 No. 11 March 2025 (4945-4961)
e-ISSN: 2798-5210
p-ISSN: 2798-5652

Study of Mohr-Coulomb Parameters in Clay Soil with the Addition of PCC Cement (Portland Cement Composite) and Lime (CAO) Under PassiveConfinement of GFRP (Glass Fiber Reinforced Polymer)

Ni Wayan Amrita Ayu Dewadatta[1]*, Laras Laila Lestari[2], Bambang Piscesa[3], Wahyuniarsih Sutrisno[4]
Institut Teknologi Sepuluh Nopember, Indonesia
Email: ayudewadattaamrita@gmail.com[1]*, laraslaila.lestari@gmail.com[2], piscesa@ce.its.ac.id[3], wahyuniarsih.its@its.ac.id[4]

**Correspondence*

ABSTRACT
This study aims to analyze the physical and mechanical behavior of soil stabilized by the addition of PCC cement and lime (CaO) and the application of passive restraint using a polymer layer strengthened by fiber glass (GFRP). Soil stabilization is carried out by mixing 8% cement and 4% lime based on the results of *the optimal mix design*. Soil specimens are compacted using standard compaction methods and tested at 28 days of age. Next, the test piece is coated with 1, 2, and 3 layers of GFRP to study the passive effect on compressive strength. The test results show that the addition of PCC cement and lime (CaO) is able to significantly increase soil strength. Mohr-Coulomb analysis showed a cohesion value of 0.032 MPa; 0.046 MPa; and 0.115 MPa, as well as deep shear angles of 45.46°, 45.08°, and 44.99° respectively for each number of GFRP layers. The application of GFRP as a passive restraint also provides a gradual increase in compressive strength according to the number of layers used. This study proves that the combination of soil stabilization using PCC cement, lime, and the application of GFRP is gradually effective in improving the physical and mechanical properties of the soil, especially for construction needs that require high bearing capacity.
Keywords: *cement treated soil; PCC;* Lime; passive restraint; triaxial.

INTRODUCTION

Soft clay soils, which are characterized by high moisture content, low carrying capacity, and significant declines, pose a major challenge in construction around the world. In regions with rapid infrastructure development, such as Southeast Asia including Indonesia, problems related to clay soils pose a major risk to structural integrity. Global efforts to address these challenges focus on environmentally friendly and cost-effective soil stabilization techniques. Cement-treated soil (CTS) and chemical stabilization involving materials such as Portland Composite Cement (PCC) and lime have emerged as important innovations in improving the physical and mechanical properties of soft clay soils (Refmasita et al., 2020).

Some of the factors that affect the problem of soft clay soil include high plasticity, low permeability, and significant development and shrinkage due to changes in moisture content (Bowles, 1996). In tropical areas with high rainfall, water infiltration further exacerbates the instability of clay soils, which often leads to structural deformations. Additionally, traditional construction practices often neglect sophisticated tillage, creating long-term maintenance issues. Reliance on conventional

stabilizers such as pure cement also increases carbon emissions, so more sustainable alternatives such as PCC are needed (Coayla & Yanati, 2023).

The impact of this problem is very wide. Low bearing capacity leads to uneven decline and premature structural failure, while rising maintenance and rehabilitation costs become a burden on construction budgets. Improper stabilization practices also contribute to ecological imbalances, which further emphasizes the importance of environmentally friendly engineering solutions. In addition, inadequate soil strength hampers project schedules, especially in large-scale development, thus affecting economic progress.

This study focuses on the use of CTS with PCC and lime (CaO) for soil stabilization, by emphasizing passive constraints using Glass Fiber Reinforced Polymer (GFRP). CTS is a widely recognized technique that combines soil, cement, and water to increase soil strength (H. Jiang, 2018). PCC, as a hydraulic cement, contains additional inorganic materials that improve its environmental profile and economic feasibility (SNI 15-7064-2004). Lime, as a traditional stabilizer, reacts with clay minerals to form long-lasting compounds, increasing soil stiffness and reducing plasticity. GFRP provides a novel approach to passive restraint, offering increased axial strength and strain control, complementing chemical stabilization methods (J. Jiang et al., 2017).

The urgency of this research comes from the urgent need to improve soil stabilization methods for sustainable infrastructure development. Indonesia's rapid urbanization and increasing demand for infrastructure highlight the important role of durable and environmentally friendly construction practices. Soft clay soils, which are widely found on construction sites, threaten the sustainability and safety of infrastructure such as roads, bridges, and foundations. This research addresses this challenge by providing practical solutions that provide measurable environmental benefits, ensuring a balance between development and sustainability.

This study aims to analyze the physical and mechanical behavior of CTS stabilized with PCC and lime, compare the results with unstabilized soil, and determine the optimal composition to achieve maximum free compressive strength (UCS). By integrating GFRP as a passive constraint method, this study evaluates improved soil stability under various load conditions. These findings are expected to provide reliable data for engineers, encourage sustainable construction practices, and contribute significantly to the advancement of geotechnical engineering.

METHOD

This study uses a qualitative approach with a descriptive method to explore and analyze in depth the physical and mechanical behavior of Cement Treated Soil (CTS) stabilized with Portland Composite Cement (PCC) and lime (CaO). The research was conducted at the Laboratory of Soil and Rock Mechanics, Faculty of Civil Engineering, Sepuluh Nopember Institute of Technology (ITS), Surabaya, Indonesia, for six months. This location was chosen because of the adequate facilities to conduct various soil tests in a controlled manner. The scope of the study includes the analysis of physical parameters such as Atterberg limits, specific gravity, and moisture content, as well as mechanical parameters such as Unconfined Compressive Strength (UCS) and soil cohesion with the Mohr-Coulomb approach.

The research population is soft clay soil found in the Surabaya area, with samples taken from a depth of 0.5 meters in the ITS Campus Robotics Field. This study involved 30 specimens with variations in the composition of PCC (4%, 8%, and 12%) and lime (0%, 4%, and 8%) to evaluate the effect of stabilization on soil strength. The research instruments include liquid and plastic limiting devices for testing physical properties, UCS tools for compression tests, and Glass Fiber Reinforced Polymer

(GFRP) as a passive restraint method. The research strategy includes literature study, sampling, laboratory testing, data analysis, and validation of results to ensure relevant solutions to soft clay soil problems.

RESULTS AND DISCUSSION

From the research conducted in the Soil and Rock Mechanics laboratory, Faculty of Civil Engineering and Planning, ITS, the results of the physical properties of clay soil were obtained, namely: moisture content (w), specific gravity (G_s), volume weight (γ_t), shrinkage limit (SL), platis limit (PL), plasticity index (PI), liquid limit (LL), and analysis of soil grain distribution. The results of the original soil experiment can be seen in Table 1.

Table 1 Data on the physical properties of the original clay soil in the yard of the ITS robotics faculty

It	Physical Properties	Result
1	Moisture content; ()W_c (%)	69.16
2	Specific gravity; () (%)G_s	2.613
3	Volume weight; () ()$\gamma gram/cm^3$	1.487
4	UCS undisturbed, ()kg/cm^3	0.226
5	Shrinkage limit; SL (%)	42.86
6	Plastic boundary; PL (%)	39.81
7	Plasticity index; PI (%)	60.15
8	Liquid limit; LL (%)	99.96
9	USCS Classification	CH
10	AASHTO Classification	A-7
11	Clay soil (%)	66.17
12	Silt land (%)	33.07
13	Sand (%)	0.76
14	Gravel (%)	0
15	OMC, (%)W_{opt}	27.50
16	MDD, ()$\gamma_{dmax} gram/cm^3$	1.150
17	California Bearing Ratio Lab, CBR (%)	0.616

Source: Testing in the Laboratory of soil and rock mechanics

Information:
OMC: Optimum Moisture Content
MDD: Maximum Dry Density

Stabilized Soil

Table 2 is the result of research conducted in the Soil and Rock Mechanics laboratory of the Faculty of Civil Engineering and ITS Planning, obtained the results of the physical properties of the

stabilized soil, namely: moisture content (w), specific gravity (G_s), dry volume weight (γ_d), shrinkage limit (SL), platis boundary (PL), plasticity index (PI), and liquid limit (LL).

Table 2
Data on the physical properties of clay soil stabilized with cement and lime

It	Test Specimen Name	Moisture Content ()W_c	Specific Gravity ()G_s	Dry Volume Weight ()γ_d	Shrink Limit (SL)	Plastic Boundary (PL)	Liquid Limit (LL)	Plasticity Index (PI)
1	C6	48.150	2.616	1.098	32.189	47.11	98.51	51.40
2	C8	41.884	2.620	1.174	38.332	47.94	98.39	50.45
3	C10	39.000	2.629	1.213	45.139	48.26	98.15	49.89
4	C12	37.025	2.675	1.241	49.869	48.40	94.09	45.68
5	C4L8	36.227	2.692	1.250	55.768	49.66	89.35	39.69
6	C8L4	35.062	2.708	1.269	56.044	50.37	85.84	35.47

Source: Testing in the Laboratory of soil and rock mechanics.

Information:
C6: Test specimen with the addition of cement at 6% of the dry weight of the soil
C8: Test specimen with additional cement of 8% of the dry weight of the soil
C10: Test specimen with the addition of cement at 10% of the dry weight of the soil
C12: Test specimen with the addition of cement at 12% of the dry weight of the soil
C4L8: Test specimen with the addition of 4% cement and 8% lime of the dry weight of the soil
C8L4: Test specimen with 8% cement and lime 4% of the dry weight of the soil

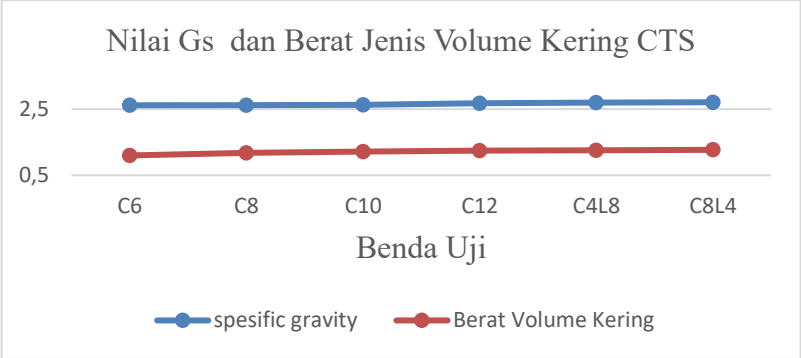

Figure 1 The relationship between specific gravity and dry volume weight to the percentage of cement and lime mixture (Author, 2024)

From the results of the physical property test of the stabilized soil, it shows that the greater the addition of cement and lime (C8L4), the higher the specific gravity value of 3.5% of the natural soil, which can be seen in Figure 1. This is because cement and lime mixed with the soil result in the process of exchanging alkaline cations (NA+ and K+) from the soil replaced by cations from cement so that the size of the clay grains increases (*flocculation*). Meanwhile, in the dry volume weight, the addition of cement and clay lime has increased, which leads to the filling of pore spaces, more efficient compaction, and the formation of denser soil structures through chemical reactions.

The porosity and pore number decreased as can be seen in figure 2. Where it indicates that the soil becomes denser and stronger, which is usually desirable in civil engineering applications such as road and foundation construction.

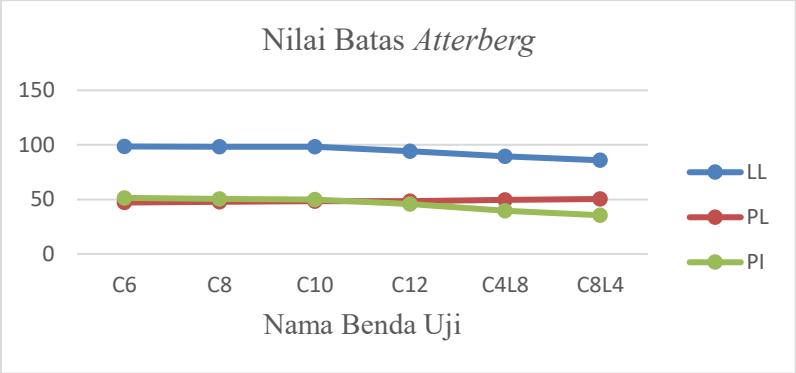

Figure 2 Relationship of Atterberg boundary to the percentage of cement and lime mixture (Author, 2024)

In Figure 2, the results of the test of the physical properties of the stabilized soil show that the greater the addition of cement and lime (C8L4), the smaller the liquid limit value (LL) decreases by 16.45%. The addition of cement and lime to the clay soil prevents the attraction process between the anions of the absorbed water particles surrounding the other clay particles, so that the clay particles lose some of the attraction between the particles, and the soil is easier to close the gap during the liquid boundary test. In the plastic limit (PL) value, it was found that the greater the addition of cement and lime (C8L4), the greater the plastic limit value (PL) increased by 20.96%. This is due to the reduction of bonds between grains, so the soil needs additional water to maintain its plasticity. Meanwhile, the value of the plasticity index (IP) decreased by 69.58%, this shows that the moisture range in which the soil remains plastic has decreased (Firoozi et al., 2017). This reflects the changes in the mechanical and chemical properties of the clay soil after the addition of cement and lime, which makes the soil more stable and less plastic.

Standard Compaction (*Proctor Standard*)

This test was carried out to find the relationship between the optimum moisture content and the dry density of the soil () or called ZAV (γ_d*Zero Air Void*) to evaluate the soil meeting the density requirements (Miswar et al., 2017). From the results of the standard compaction test of a mixture of clay soil with cement and lime with a composition of 12% cement, 8% cement 4% lime, and 4% lime 8% cement, the optimum moisture content (OMC) value and maximum dry fill weight () were obtained as shown in table 3.γ_d

Table 3 Results of testing the dry volume weight value and optimum moisture content in a clay soil mixture with the addition of cement and lime

It	Test Specimen Name	Dry Volume Weight ()γ_d	Optimum Water Rate ()w_{opt}	γ_d / w_{opt}
1	C12	1.280	37.50	0.0341
2	C8L4	1.257	38.00	0.0331
3	C4L8	1.241	38.50	0.0322

Source: Testing in the Laboratory of mechanics and rocks

Information:

C12: Test specimen with the addition of cement at 12% of the dry weight of the soil

C4L8: Test specimen with the addition of 4% cement and 8% lime of the dry weight of the soil
C8L4: Test specimen with 8% cement and lime 4% of the dry weight of the soil

In the standard compaction test, it was found that the ratio of dry volume weight to optimum moisture content decreased when the lime mixture was more than cement.

***California Bearing Ratio* (CBR)**

CBR (*California Bearing Ratio*) is a test to determine the type of pavement layer to be produced. In the CBR test, the laboratory mixed clay soil with cement and lime with the composition of each mixture, namely cement 6%, 8%, 10%, 12%, cement 4%, lime 8%, and cement 8% lime 4%. This uses a 4-day curing period obtained from the Laboratory CBR value as shown in table 4.

Table 4
CBR value test results of laboratory mixture of clay soil with cement and lime

It	Test Specimen Name	CBR Soaked	Layer Type
1	C6	2.163	*Sub grade*
2	C8	12.185	*Sub-base*
3	C10	13.260	*Sub-base*
4	C12	14.514	*Sub-base*
5	C4L8	17.739	*Sub-base*
6	C8L4	22.655	*Sub-base*

Source: Testing in the Laboratory of mechanics and rocks

Information:
C6: Test specimen with the addition of cement at 6% of the dry weight of the soil
C8: Test specimen with additional cement of 8% of the dry weight of the soil
C10: Test specimen with the addition of cement at 10% of the dry weight of the soil
C12: Test specimen with the addition of cement at 12% of the dry weight of the soil
C4L8: Test specimen with the addition of 4% cement and 8% lime of the dry weight of the soil
C8L4: Test specimen with 8% cement and lime 4% of the dry weight of the soil

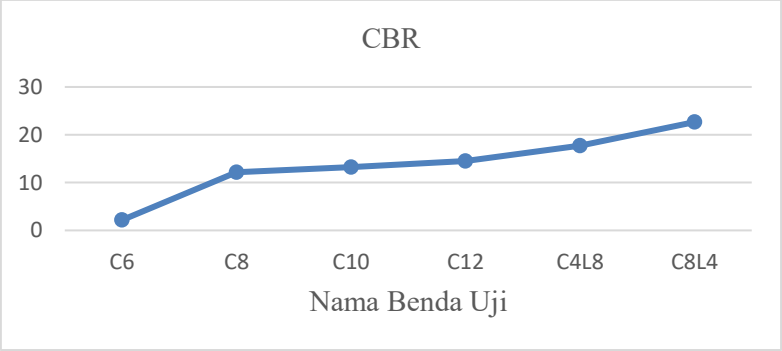

Figure 3 Relationship of Laboratory CBR value to clay soil mixture with the addition of cement and lime

Figure 3 shows that the greater the addition of cement and lime, the higher the CBR value of clay soil, this is because cement and lime mixed with soil result in the process of exchange of alkaline cations (Na+ and K+) from the soil replaced by cations from cement so that the size of clay grains increases (*flocculation*). In addition to *the flocculation* that occurs in the pozzolan process, hydration and

cementation also occur. The pozzolan process occurs between calcium hydroxide from the soil reacting with silicate (SiO2) and aluminate (AlO3) from cement to form a binding material consisting of calcium silicate or aluminate silicate. The reaction of Ca^{2+} with silicates and aluminates from the surface of the clay particles forms a cement paste (*hydrated gel*) so that it binds the clay particles.

The results of the experiment showed that starting with the addition of 6% cement including the *subgrade* layer, then the addition of 8%, 10%, and 12% cement including the subbase layer, and C4L8 and C8L4 also included the subbase layer.

Curing 28 days

In Figure 4, the CTS with a 1-layer GFRP constraint experiences an elastic phase from the beginning of loading until the stress reaches 2.116 MPa and the strain reaches 0.0076. In this phase, the lines on the curve are linear, which shows a proportional relationship between stress and strain. During the elastic phase, the material can return to its original shape if the load is removed and does not suffer damage.

The tension-strain relationship is linear at the beginning of the curve, showing the elastic deformation of the material according to Hooke's Law. The elastic modulus (E) of the material in the test of 278.42 MPa indicates the stiffness of the material to elastic deformation under compressive loads. According to (Davis et al., 2019), lightweight construction materials intended to withstand compressive loads have a moderate modulus of elasticity.

Then, there is a transition from the elastic phase to the plastic phase, which is characterized by a hardening curve. Cracks begin to occur causing the accumulation of plastic deformation. This indicates that the material has passed its elastic capacity and is subjected to permanent plastic deformation or cannot return to its original shape. In this phase, microscopic damage such as the rupture of the binding matrix causes a decrease in strength and changes in the deformation characteristics of the material. This *hardening* phase continues until the peak point or maximum compressive strength with a stress of 9.275 MPa and a strain of 0.038.

At the peak point, the material experiences *sudden failure*, which can be seen from the sharp jump of voltage drop. *Sudden failure* occurs because internal cracks in the material develop and spread rapidly and the material experiences a decrease in strength and so that the load exceeds the strength capacity of the material (Moeinabadi-Bidgoli et al., 2023). The stress decreases to 7.694 MPa and the strain increases to 0.039.

After experiencing *a sudden failure*, the material again experienced a slow decrease in stress. This lasts until the stress reaches a value of 3.926 Mpa and the strain value of 0.0396. At this time, the material enters the residual phase, where the voltage drops so little that in this phase, the lines on the curve are relatively linear and flat. Residual stress occurs as a result of the use of constraints on the material which causes a change in the voltage distribution in the material resulting in residual stress in this phase.

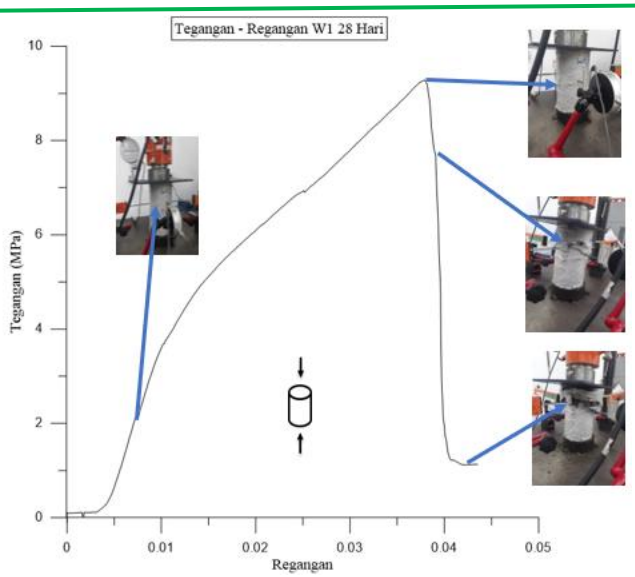

Figure 4
Tension and Strain Relationship CP_W1_28 days

This residual phase lasts until the test sample reaches its final condition, at which point the curve no longer shows a significant load drop. This final condition was reached at a stress of 1.119 MPa and a strain of 0.042, indicating that the material had reached its permanent deformation limit. The residual phase provides important information about the behavior of the material after failure, which is useful for understanding the durability and durability of the material in the long term.

Curing 7 days

In Figure 5, the CTS with a 3-layer GFRP constraint experiences an elastic phase from the beginning of loading until the stress reaches 4.438 MPa and the strain reaches 0.026. At this stage, the curve shows a straight line that depicts the relationship between tension and strain. During the elastic phase, the material can return to its original shape if the load is removed without experiencing damage.

The tension-strain relationship is linear at the beginning of the curve, showing the elastic deformation of the material according to Hooke's Law. The elastic modulus (E) of the material in the test of 170.692 MPa indicates the stiffness of the material to elastic deformation under compressive loads. According to (Davis et al., 2019), lightweight construction materials intended to withstand compressive loads have a moderate modulus of elasticity.

Then, there is a transition from the elastic phase to the plastic phase, which is characterized by a hardening curve. Cracking begins to occur, which leads to increased plastic deformation. This indicates that the material has passed its elastic capacity and undergone permanent plastic deformation, so it cannot return to its original shape. At this stage, microscopic damage such as the rupture of the binding matrix occurs, resulting in a decrease in strength as well as changes in the deformation characteristics of the material (Mehta & Monteiro, 2014). This hardening phase continues until the peak point or maximum compressive strength with a stress of 15.156 MPa and a strain of 0.115.

At the peak point, the material experiences *sudden failure*, which can be seen from the sharp jump of voltage drop. *Sudden failure* occurs due to internal cracks in the material that develop and spread rapidly, and the material experiences a decrease in strength so that the load exceeds the strength capacity of the material (Moeinabadi-Bidgoli et al., 2023). The stress decreases to 9.207 MPa and the

strain increases to 0.146. This phase indicates that the material is no longer able to withstand the additional load, and the internal structure of the material begins to deteriorate.

After experiencing *a sudden failure*, the material again experienced a slow decrease in stress. This lasts until the stress reaches a value of 8.484 Mpa and the strain value is 0.120. At this time, the material enters the residual phase, where the voltage drops so little that in this phase, the lines on the curve are relatively linear and flat. Residual stress occurs due to the use of constraints on the material, which changes the distribution of stress in the material resulting in the occurrence of residual stress in that phase.

This residual phase lasts until the test sample reaches its final condition, at which point the curve no longer shows a significant load drop. This final condition was reached at a stress of 2.312 MPa and a strain of 0.165, indicating that the material had reached its permanent deformation limit. The residual phase provides important information about the behavior of the material after failure, which is useful for understanding the durability and durability of the material in the long term.

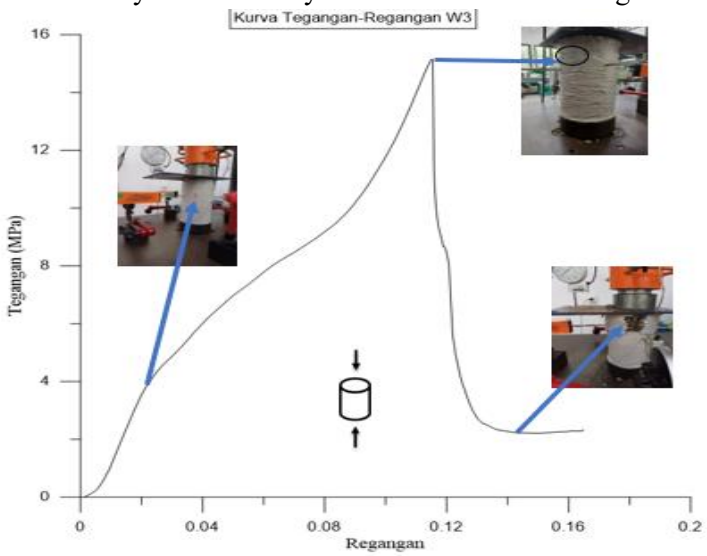

Figure 5
Tension and strain relationship CP_W3_7 days

Curing 28 days

In Figure 5, the CTS with a 3-layer GFRP constraint undergoes an elastic phase from the beginning of loading until the stress reaches 4.031 MPa and the strain reaches 0.012. At this stage, the curve shows a straight line that depicts the relationship between tension and strain. During the elastic phase, the material can return to its original shape if the load is removed without experiencing damage (Neville, 2011).

The tension-strain relationship is linear at the beginning of the curve, showing the elastic deformation of the material according to Hooke's Law. The elastic modulus (E) of the material in the test of 335.92 MPa indicates the stiffness of the material against elastic deformation under compressive loads. According to Davis et al. (2019), lightweight construction materials intended to withstand compressive loads have a moderate modulus of elasticity.

Then, there is a transition from the elastic phase to the plastic phase, which is characterized by a hardening curve. Cracking begins to occur, which leads to increased plastic deformation. This indicates that the material has passed its elastic capacity and undergone permanent plastic deformation, so it

cannot return to its original shape (Celik et al., 2014). At this stage, microscopic damage such as the rupture of the binding matrix occurs, resulting in a decrease in strength as well as changes in the deformation characteristics of the material. This *hardening* phase continues until the peak point or maximum compressive strength with a stress of 19.065 MPa and a strain of 0.110. At the peak point, the material experiences *sudden failure*, which can be seen from the sharp jump of voltage drop. *Sudden failure* occurs due to internal cracks in the material that develop and spread rapidly, and the material experiences a decrease in strength so that the load exceeds the strength capacity of the material. The stress decreases to 9.453 MPa and the strain increases to 0.118. This phase indicates that the material is no longer able to withstand the additional load, and the internal structure of the material begins to deteriorate.

After experiencing *a sudden failure*, the material again experienced a slow decrease in stress. This lasts until the stress reaches a value of 4.978 Mpa and the strain value is 0.148. At this time, the material enters the residual phase, where the voltage drops so little that in this phase, the lines on the curve are relatively linear and flat. Residual stress occurs due to the use of constraints on the material, which changes the distribution of stress in the material resulting in the occurrence of residual stress in that phase.

This residual phase lasts until the test sample reaches its final condition, at which point the curve no longer shows a significant load drop. This final condition was reached at a stress of 2.399 MPa and a strain of 0.207, indicating that the material had reached its permanent deformation limit. The residual phase provides important information about the behavior of the material after failure, which is useful for understanding the durability and durability of the material in the long term.

Volumetric strain analysis

The analysis of volumetric strain in CTS with GFRP constraints was carried out to determine the behavior of material volumetric changes and their relationship in determining the original peak voltage of CTS with GFRP constraints. In constrained materials such as CTS with GFRP constraints, there is often confusion in determining the peak voltage, because the collapse that occurs during the test is a failure of the GFRP constraint, while the CTS material has collapsed first.

This analysis aims to determine the original value of the peak voltage at the CTS with GFRP constraints by considering parameters such as volumetric strain and axial strain.

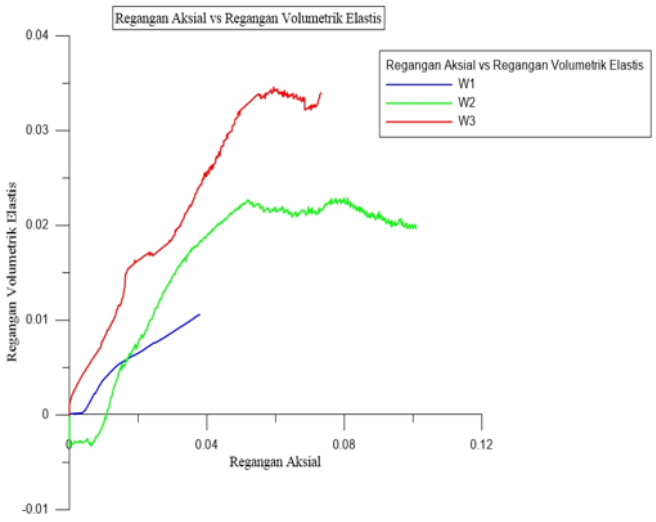

Figure 6Relationship curve between *elastic volumetric strain* and *axial strain* with *28-day* curing

Figure 6 is the relationship curve between *elastic volumetric strains* and *axial strains*. *Elastic volumetric strain* is a temporary volume change when the material receives a load, then it will return to its initial shape after the load is removed. Meanwhile, plastic volumetric strain is a change in volume in a material when the load exceeds its elastic limit so that the volume change that occurs is fixed and does not return to its original shape even though the load has been removed.

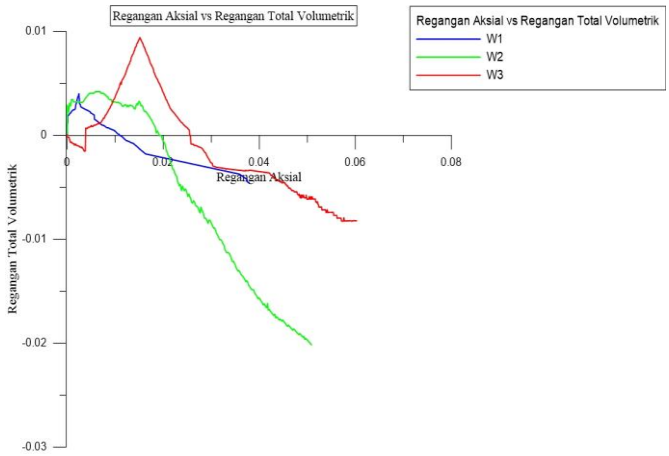

Figure 7 Total volumetric strain curve with axial strain

In Figure 7, the total volumetric strain curve against axial strain is presented. Total volumetric strain is the sum of elastic and plastic volumetric strains in axial and lateral directions. In all three variations in the number of GFRP layers, the curve shows the presence of a compact that occurs from the beginning to the axial strain values of 0.0109, 0.0192 and 0.0255 for 1, 2, and 3 layers of GFRP respectively. After the compaction occurs, the material undergoes a decrease in volumetric strain.

In the designated section, it can be seen that axial strain at peak time occurs when the total volumetric strain is equal to zero. This is in line with (Piscesa et al., 2017) which states that the total volumetric strain is zero at peak stress, At the beginning of load application until before peak stress, the material undergoes commotion until the plastic phase. When the stress reaches its peak, the GFRP constraint begins to tear so that the CTS material will undergo *dilation* because the constraint is no longer able to withstand the lateral expansion of the load.

Peak elastic volumetric strain on CTS with GFRP constraints

1. Wrap 1

Peak elastic volumetric strain is an important parameter in determining the original peak stress at the CTS with GFRP constraints. The peak elastic volumetric strain is obtained from the relationship curve between elastic volumetric strain and axial strain and total volumetric strain with axial strain. The peak elastic volumetric strain is the value of elastic volumetric strain when the total volumetric strain is equal to 0.

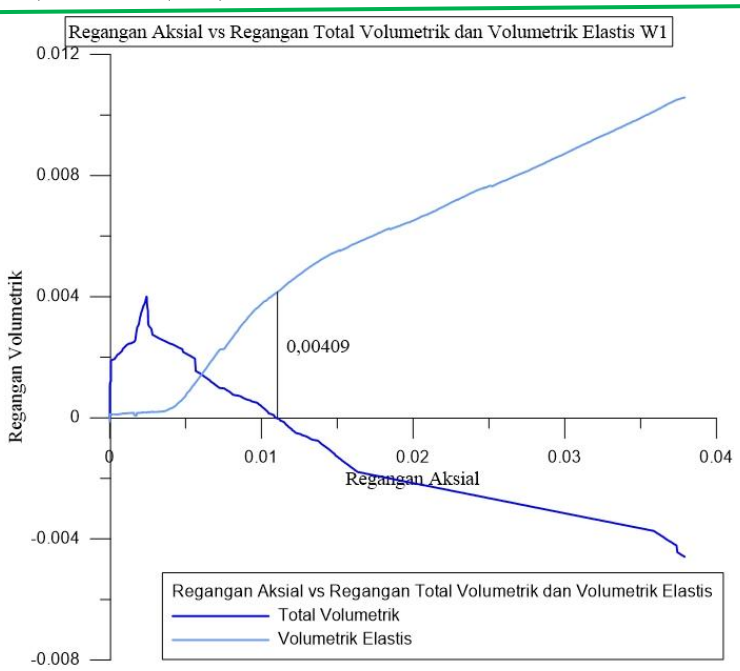

Figure 8

Total and elastic volumetric strain vs axial strain W1

In Figure 8, it can be seen that the total volumetric strain is 0 at an axial strain value of -0.00409. At this strain value, an elastic volumetric strain value of 0.0109 was obtained. This value is the value of the peak elastic volumetric strain on the CTS with a 1-layer GFRP constraint.

2. Wrap 2

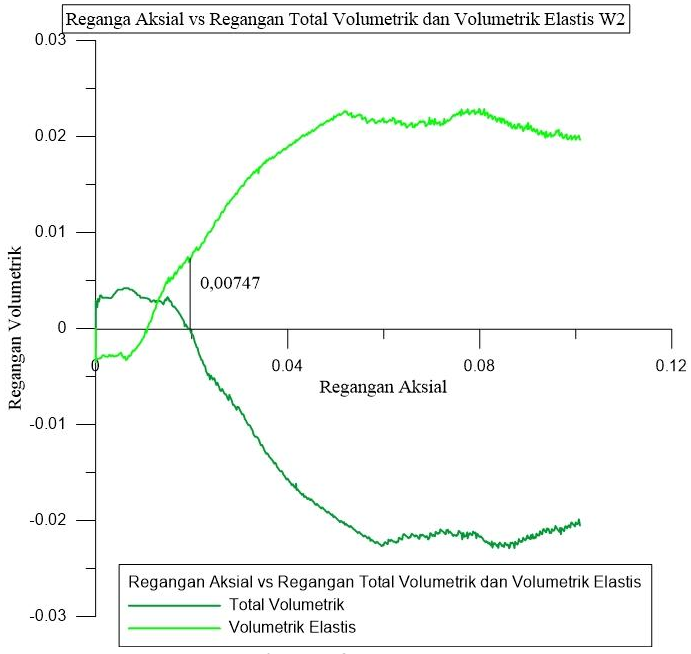

Figure 9

Total and elastic volumetric strain vs axial strain W2

In Figure 9, it can be seen that the total volumetric strain is 0 at the axial strain value of -0.00747. At the strain value, an elastic volumetric strain value of 0.0192 was obtained. This value is the value of the peak elastic volumetric strain on the CTS with a 2-layer GFRP constraint.

3. Wrap 3

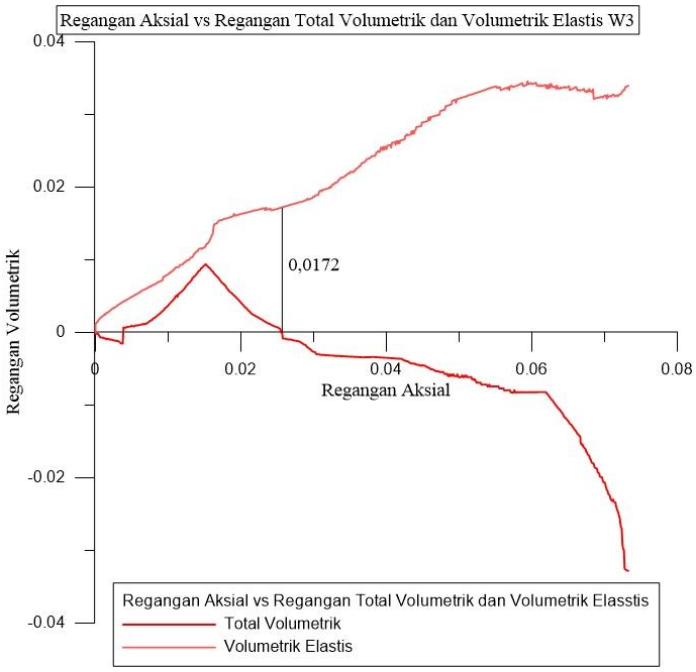

Figure 10
Total and elastic volumetric strain vs axial strain W3

In Figure 10, it can be seen that the total volumetric strain is 0 at an axial strain value of -0.0172. At this strain value, an elastic volumetric strain value of 0.0255 was obtained. This value is the value of the peak elastic volumetric strain on the CTS with a 3-layer GFRP constraint.

Analysis of Mohr Coulomb's criteria using *the Stress Path method*

The Mohr-Coulomb theory is used to describe the strength and stability of a material, where this theory states that material collapse occurs when the shear stress on the material reaches the maximum value determined by the normal stress and the shear force of the material *stress path* is a graph that shows the change in stress received by a material during the testing process or changes in load conditions (Touhari & Mitiche-Kettab, 2016). *The stress path* describes how normal stresses and shear stresses change over time or change conditions. Stress path analysis was used to determine the Mohr Coulomb criteria, namely cohesion parameters (c) and soil shear angle (ϕ) (Das, 2011). The stress path has output parameters in the form of α the slope of the failure envelope and c cot ϕ at the intersection of the failure envelope with the q-axis. Cohesion (c) and the shear angle of the ground (ϕ) will be obtained by applying equations 2.11 – 2.19. Table 4.8 shows the results of the analysis of *the Mohr Coulomb* criteria using *the stress path* method.

Table 5
Criteria for *mohr coulomb*

Variations	GFRP (*ply*)	k	ϕ	*d*	*c*
W1	1	4,96	45,46	0,02	0,032

W2	2	4,85	45,08	0,03	0,046
W3	3	4,83	44,99	0,08	0,115

The analysis of *stress paths* in CTS with GFRP constraints of 1, 2, and 3 layers is discussed further in sub chapters 4.7.1-4.7.3.

***CTS Stress Path* with 1-layer GFRP constraint**

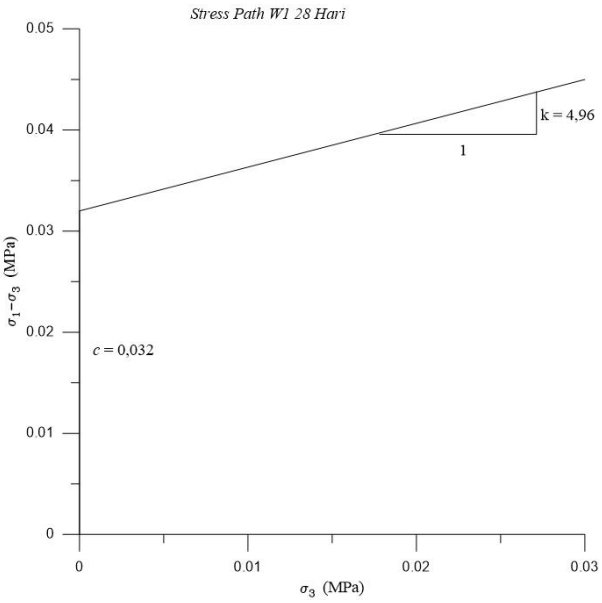

Figure 11
***Stress path* W1 28 days**

From the analysis of the stress path on CTS with a 1-layer GFRP constraint as shown in Figure 11, it can be seen that the k value formed between the stress path and the horizontal direction has a value of 4.96. This value will be used to find out the magnitude of the shear angle (ϕ) by entering it in equation 2.18 so that a value ϕ of 45.46° is obtained. This value is greater than the range of shear angle values for cement soil mixtures, which is 20 - 35° . Meanwhile, it is also known from the figure that *the stress path* intersects with the axis with a value of 0.023. This value is the value of $\sigma_1 - \sigma_3 d$. With this value, the cohesion amount c is obtained as 0.032 MPa. The cohesion value obtained is smaller than the cohesion value range for cement soil mixtures, which is 0.05-0.15 MPa. Large shear angles and cohesion indicate a strong soil ability to withstand shear loads.

***CTS Stress Path* with 2-layer GFRP constraints**

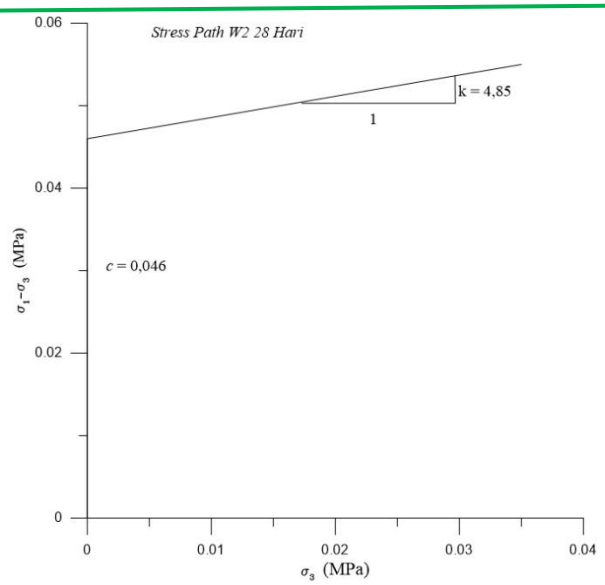

Figure 12 *W2 stress path* 28 days

From the analysis of the stress path on CTS with a 1-layer GFRP constraint as shown in Figure 12, it can be seen that the k value formed between the stress path and the horizontal direction has a value of 4.85. This value will be used to find out the magnitude of the shear angle (ϕ) by entering it in equation 2.18 so that a value ϕ of 45.08° is obtained. This value is greater than the range of shear angle values for cement soil mixtures, which is 20 - 35°. Meanwhile, it is also known from the figure that *the stress path* intersects with the axis with a value of 0.033. This value is the value of $\sigma_1 - \sigma_3 d$. With this value, the cohesion of c is obtained as 0.046 MPa. The cohesion value obtained is smaller than the cohesion value range for cement soil mixtures, which is 0.05-0.15 MPa. Large shear angles and cohesion indicate a strong soil ability to withstand shear loads.

***Stress Path* CTS with 3-layer GFRP constraints**

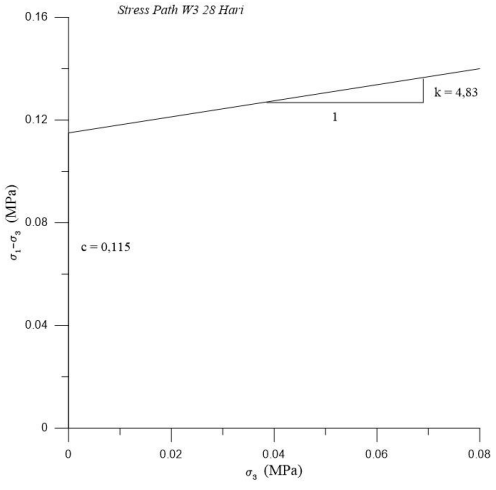

Figure 13 *W3 28-day* stress path

From the analysis of the stress path on CTS with a 1-layer GFRP constraint as shown in Figure 13, it can be seen that the k value formed between the stress path and the horizontal direction has a value of 4.83. This value will be used to find out the magnitude of the shear angle (ϕ) by entering it in equation 2.18 so that a value ϕ of 44.99° is obtained. This value is greater than the range of shear angle values for cement soil mixtures, which is 20 - 35°. Meanwhile, it is also known from the figure that *the stress path* intersects with the axis with a value of 0.081. This value is the value of $\sigma_1 - \sigma_3 d$. With this value, the cohesion of c is obtained as 0.115 MPa. The cohesion value obtained satisfies the cohesion value range for cement soil mixtures, which is 0.05-0.15 MPa. Large shear angles and cohesion indicate a strong soil ability to withstand shear loads (Horpibulsuk et al., 2005).

CONCLUSION

From the results of the research and analysis that has been carried out, it is obtained that Cement-lime Treated Soil (CTS) with the passive constraint of Glass Fiber Reinforced Polymer (GFRP) has great potential in improving the stability of soft clay soils. The optimum composition of the material was found in the use of PCC of 8% and lime of 4% of the dry soil weight, with a curing time of at least 28 days to achieve optimal strength. The results showed that the variation of CTS C8L4 (PCC 8% + lime 4%) resulted in a significant improvement in soil physical and mechanical parameters, including a decrease in moisture content of up to 97%, an increase in specific gravity to 3.5%, and an increase in the compressive strength value with the highest compressive strength in a test specimen with a 3-layer GFRP passive constraint of 19.065 MPa. In addition, the addition of GFRP was shown to increase elastic volumetric strain and material capacity in withstanding axial loads. With these results, the CTS approach with GFRP becomes an innovative solution to improve the quality of soft clay soils in sustainable construction applications.

BIBLIOGRAPHY

Celik, K., Jackson, M. D., Mancio, M., Meral, C., Emwas, A.-H., Mehta, P. K., & Monteiro, P. J. M. (2014). High-volume natural volcanic pozzolan and limestone powder as partial replacements for portland cement in self-compacting and sustainable concrete. *Cement and Concrete Composites*, *45*, 136–147.

Coayla, P., & Yanati, K. (2023). *El nivel de exportaciones tradicionales y su relación con el crecimiento de la economía China, periodo 2012-2021*.

Davis, D., Massinger, T., Lundgren, A., Driggers, J. C., Urban, A. L., & Nuttall, L. (2019). Improving the sensitivity of Advanced LIGO using noise subtraction. *Classical and Quantum Gravity*, *36*(5), 55011.

Firoozi, A. A., Guney Olgun, C., Firoozi, A. A., & Baghini, M. S. (2017). Fundamentals of soil stabilization. *International Journal of Geo-Engineering*, *8*, 1–16.

Jiang, H. (2018). Simple three-dimensional Mohr-Coulomb criteria for intact rocks. *International Journal of Rock Mechanics and Mining Sciences*, *105*, 145–159.

Jiang, J., Xiao, P., & Li, B. (2017). True-triaxial compressive behaviour of concrete under passive confinement. *Construction and Building Materials*, *156*, 584–598.

Miswar, M., Syaifuddin, S., & Amani, N. (2017). Stabilisasi Tanah Lempung Menggunakan Semen Dan Kapur Untuk Meningkatkan Daya Dukung Cbr Tanah. *Portal: Jurnal Teknik Sipil*, *9*(2).

Moeinabadi-Bidgoli, K., Rezaee, M., Hossein-Khannazer, N., Babajani, A., Aghdaei, H. A., Arki, M. K., Afaghi, S., Niknejad, H., & Vosough, M. (2023). Exosomes for angiogenesis induction in ischemic disorders. *Journal of Cellular and Molecular Medicine*, *27*(6), 763–787.

Piscesa, B., Attard, M. M., & Samani, A. K. (2017). Three-dimensional finite element analysis of circular reinforced concrete column confined with FRP using plasticity model. *Procedia Engineering*, *171*, 847–856.

Refmasita, A. N., Amar, F., & Larasati, M. (2020). Label Halal dan Kualitas Produk Obat terhadap Minat Beli Obat pada Mahasiswa Feb Uhamka. *Al-Urban*, *4*(2), 168–179.

Touhari, M., & Mitiche-Kettab, R. (2016). Behaviour of FRP confined concrete cylinders: Experimental investigation and strength model. *Periodica Polytechnica Civil Engineering*, *60*(4), 647–660.